

---

## PHYSICS OF SEMICONDUCTOR DEVICES

---

# The Resonant Terahertz Response of a Slot Diode with a Two-Dimensional Electron Channel<sup>1</sup>

V. V. Popov<sup>1^</sup>, G. M. Tsymbalov<sup>1</sup>, M. S. Shur<sup>2</sup>, and W. Knap<sup>2,3</sup>

<sup>1</sup>*Institute of Radio Engineering and Electronics, Saratov Division,  
Russian Academy of Sciences, Saratov, 410019 Russia*

<sup>^</sup>*e-mail: popov@ire.san.ru*

<sup>2</sup>*Department of Electrical, Computer, and System Engineering and RPI/IBM Center  
for Broadband Data Transfer, CII9015, Rensselaer Polytechnic Institute, Troy, New York, 12180 USA*

<sup>3</sup>*GES CNRS-Universite Montpellier2 UMR 5650, 34900 Montpellier, France*

Submitted June 1, 2004; accepted for publication June 14, 2004

**Abstract**—The terahertz response of a slot diode with a two-dimensional electron channel is calculated on the basis of the first principles of electromagnetism. It is shown that all characteristic electromagnetic lengths (scattering, absorption, and extinction lengths), as well as the impedance of the diode, exhibit resonances at plasmon excitation frequencies in the channel. The fundamental resonance behaves similarly to the current resonance in an *RLC* circuit. It has been concluded that, even at room temperature, a slot diode with a two-dimensional electron channel provides a resonant circuit at terahertz frequencies that couples effectively to external electromagnetic radiation with a loaded *Q*-factor exceeding unity. The diode resistance may be measured from contactless measurements of the characteristic electromagnetic lengths of the diode. © 2005 Pleiades Publishing, Inc.

## 1. INTRODUCTION

The high-frequency response of field-effect transistors and diodes with two-dimensional electron channels is strongly affected by plasma oscillations in the channel. This phenomenon, in its various manifestations, can be used for the detection, frequency multiplication, and generation of terahertz (THz) radiation [1–13]. One of the main parameters of a device, which determines its high frequency properties, is the device impedance. The high-frequency impedance (admittance) of a slot diode was calculated for a capacitively [14] and conductively [15] contacted two-dimensional electron channel. This was performed within the framework of electrostatic theory and an equivalent circuit approach. In these approaches, the radiative contribution to the impedance (radiation resistance  $R_{\text{rad}}$  of the diode) is not considered, and intercontact geometrical capacitance  $C_g$  is either ignored altogether [14] or treated as a free parameter [15]. However, at ultrahigh (terahertz) frequencies (i) the radiation resistance of the diode may play the role of an additional damping mechanism, and (ii) the intercontact geometrical capacitance may effectively shunt the channel. Furthermore, the typical length of the side contacts in high-frequency high-electron-mobility transistors (HEMT) [12] is comparable to the THz radiation wavelength, which makes the electrostatic calculations of the intercontact capacitance inaccurate. Here we calculate the impedance of a slot diode with a conductively contacted two-dimensional electron channel using the full system of Maxwell's

equations. In this way, we account for the radiation resistance and intercontact capacitance from first principles. In addition to its practical importance, the slot diode analyzed here is an idealization of the long ungated parts of the HEMT with an ultrashort nanometer gate. This HEMT was recently shown to exhibit a resonant THz emission that could be tuned using a bias voltage [12].

## 2. THEORETICAL MODEL

Consider a plane electromagnetic wave incident, normally from vacuum onto a perfectly conductive plane  $z = 0$  with a slot of width  $w$ , which is located on the surface of a dielectric substrate. We assume that the electric field of the wave,  $\mathbf{E}_0 \exp(-i\omega t - ik_0 z)$  (where  $k_0 = \omega/c$  and  $c$  is the speed of light in free space), is polarized across the slot (along the  $x$ -axis). The edges of the slot are connected by a two-dimensional electron channel with the areal conductivity described by the Drude model as

$$\sigma(\omega) = i \frac{Ne^2}{m^*(\omega + i\nu)},$$

where  $\nu$  is the electron momentum scattering rate,  $N$  is the sheet electron density, and  $e$  and  $m^*$  are the charge and effective mass of electron, respectively.

Our theoretical procedure involves the following steps: We rewrite Maxwell's equations for the ambient medium and the substrate in the Fourier transform representation over the in-plane wave vector  $k_x$ . The Fou-

<sup>1</sup>This article was submitted by the authors in English.

rier transforms of the in-plane components of the electric and magnetic fields satisfy the following boundary conditions at  $z = 0$ :

$$\begin{aligned}\delta(k_x)E_0 + E_{x,a}^{(\text{ind})}(k_x) &= E_{x,s}^{(\text{tot})}(k_x), \\ \delta(k_x)H_0 + H_{y,a}^{(\text{ind})} - H_{y,s}^{(\text{tot})}(k_x) &= j(k_x),\end{aligned}$$

where  $j(k_x)$  is the Fourier transform of the surface electron current density,  $\delta(k_x)$  is the Dirac  $\delta$ -function, the subscripts  $a$  and  $s$  label the fields in the ambient medium and the substrate respectively, the superscripts (ind) and (tot) refer to induced and total fields, and  $E_0$  and  $H_0$  are the amplitudes of electric and magnetic fields in the incident wave. Then we relate the Fourier transform of the surface electron current density in the diode plane to that of the in-plane electric field in the same plane as

$$j(k_x) = G(k_x)E_x(k_x) + \frac{2}{Z_0}\delta(k_x)E_0,$$

where  $E_x(k_x) = E_{x,s}^{(\text{tot})}(k_x)$  is the Fourier transform of the in-plane component of the total electric field in the diode plane and  $Z_0$  is the free space impedance. The  $k_x$ -space surface admittance  $G(k_x)$  depends exclusively on the frequency and dielectric constants of the ambient medium  $\epsilon_a$  (which we assume to be unity) and the substrate  $\epsilon_s$ ; therefore,

$$G(k_x) = \frac{\chi_a + \chi_s}{Z_0},$$

where

$$\chi_{a(s)} = \frac{\epsilon_{a(s)}k_0}{\sqrt{k_0^2\epsilon_{a(s)} - k_x^2}}.$$

Coming back to the real-space representation we have

$$j(x) = \frac{2E_0}{Z_0} + \int_{-\infty}^{\infty} dx' E_x(x') \int_{-\infty}^{\infty} dk_x G(k_x) \exp[ik_x(x - x')].$$

Using Ohm's law  $j(x) = \sigma(\omega)E_x(x)$  for the two-dimensional electron channel and the condition  $E_x = 0$  for the perfectly conductive contact half-planes, we obtain the following integral equation for an in-plane component of the total electric field within the slot:

$$\sigma(\omega)E_x(x) = \int_{-w/2}^{w/2} G(x, x')E_x(x')dx' + \frac{2E_0}{Z_0} \quad (1)$$

with the kernel

$$G(x, x') = \int_{-\infty}^{\infty} dk_x G(k_x) \exp[ik_x(x - x')].$$

Integral Eq. (1) is solved numerically by the Galerkin method through its projection onto an orthogonal set of

Legendre's polynomials within the interval  $[-w/2, w/2]$ . As a result, we find the induced electric field in the ambient medium is

$$\mathbf{E}_a^{(\text{ind})}(\mathbf{r}) = \mathbf{E}_0 \exp(ik_0 z) + \int_{-\infty}^{\infty} \mathbf{E}_a^{(\text{sc})}(k_x) \exp(i\mathbf{k}_a \mathbf{r}) dk_x, \quad (2)$$

and the total electric field in the substrate is

$$\mathbf{E}_s^{(\text{tot})}(\mathbf{r}) = \int_{-\infty}^{\infty} \mathbf{E}_s^{(\text{sc})}(k_x) \exp(i\mathbf{k}_s \mathbf{r}) dk_x. \quad (3)$$

The electric fields  $\mathbf{E}_a^{(\text{ind})}(\mathbf{r})$  and  $\mathbf{E}_s^{(\text{tot})}(\mathbf{r})$  have zero  $y$ -components, and  $\mathbf{r}$  is the two-dimensional radius vector  $\mathbf{r} = \{x, y\}$ .

The wave vectors  $\mathbf{k}_{a(s)}$  have  $k_x$  and  $k_z = \pm \sqrt{k_0^2\epsilon_{a(s)} - k_x^2}$  as their components. The integrals on the right-hand sides of Eqs. (2) and (3) describe the scattered fields in terms of the plane-wave continuum, while the first summand in Eq. (2) is the wave reflected normally from a perfectly conductive plane. The sign before the radical, in the expression for  $k_z$ , is chosen to correspond to the outgoing waves for  $k_x < k_0\sqrt{\epsilon_{a(s)}}$  and evanescent waves for  $k_x > k_0\sqrt{\epsilon_{a(s)}}$  in the respective medium.

Since only the outgoing plane waves (with  $k_x < k_0\sqrt{\epsilon_{a(s)}}$ ) contribute to radiative losses, we can calculate the fluxes of energy scattered per unit length of the slot in each medium as

$$P_{a(s)} = \frac{\pi}{Z_0} \int_{-k_0\sqrt{\epsilon_{a(s)}}}^{k_0\sqrt{\epsilon_{a(s)}}} \mathbf{n}_{a(s)} \frac{\mathbf{k}_{a(s)}}{k_0} |\mathbf{E}_{a(s)}^{(\text{sc})}(k_x)|^2 dk_x,$$

where  $\mathbf{n}_{a(s)}$  is the internal normal to the diode plane in the respective medium. Then we can define the scattering length as  $L_{a(s)}^{(\text{sc})} = P_{a(s)}/P_0$  in each medium, where  $P_0$  is the energy flux density in the incident wave. We can also introduce the total scattering length as  $L^{(\text{sc})} = L_a^{(\text{sc})} + L_s^{(\text{sc})}$  and the absorption length as  $L^{(\text{ab})} = Q/P_0$ , where

$$Q = \frac{1}{2} \int_{-w/2}^{w/2} |E_x(x, 0)|^2 \text{Re}[\sigma(\omega)] dx$$

is the energy absorption rate (per unit length of the slot). The scattering and absorption lengths obey the energy conservation law in the form  $L^{(\text{sc})} + L^{(\text{ab})} = L^{(\text{ex})}$ , where

$$L^{(\text{ex})} = 4\pi \frac{\text{Re}[\mathbf{E}_0^* \mathbf{E}_a^{(\text{sc})}(k_x = 0)]}{|E_0|^2} \quad (4)$$

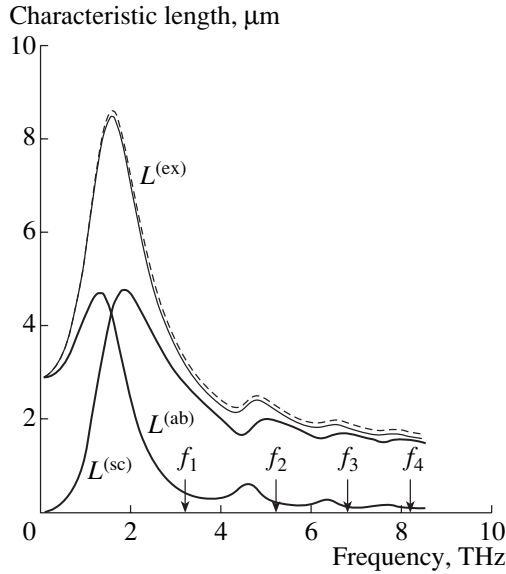


**Fig. 1.** Characteristic lengths vs. frequency for the slot diode with the parameters  $N = 3 \times 10^{12} \text{ cm}^{-2}$ ,  $v = 4.35 \times 10^{12} \text{ s}^{-1}$ ,  $w = 1.3 \text{ μm}$ ,  $\epsilon_s = 13.88$ , and  $m^* = 0.042m_0$ .

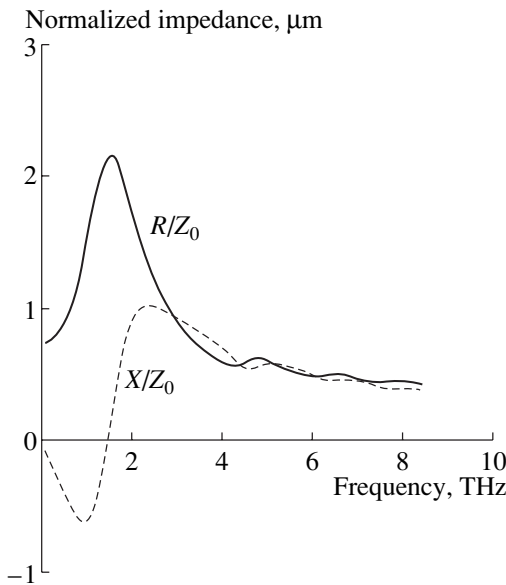


**Fig. 2.** Impedance of the slot diode with a two-dimensional electron channel vs. frequency.

is the extinction length, which is the ratio of the amount of energy picked out of the incident wave per unit time (per unit length of the slot) to that of the energy flux density in the incident wave. The formula analogous to Eq. (4) is the so-called optical theorem, in scattering theory [16].

### 3. RESULTS AND DISCUSSION

The calculated spectra of the scattering, absorption, and extinction lengths are shown in Fig. 1 for param-

eters typical of two-dimensional electron channels in gate-length HEMT of less than 100 nm at room temperature [12]. All characteristic lengths exhibit maxima at plasmon resonance frequencies in the channel. Note that, in order of magnitude, the extinction length exceeds the geometrical width of the slot even for the short electron relaxation time chosen for the calculations. The arrows in Fig. 1 mark the frequencies of ungated plasmons in an isolated two-dimensional electron channel with wave vectors  $q_n = (2n - 1)\pi/w$  ( $n = 1, 2, 3, \dots$ ), which are estimated by a simple approximate formula [17]:

$$f_n = \frac{1}{2\pi} \sqrt{\frac{e^2 N q_n}{m^* \epsilon_0 (1 + \epsilon_s)}}. \quad (5)$$

It is evident from Fig. 1 that the plasma oscillations in the slot diode are softened because of the induction of image charges by these oscillations in the perfectly conductive contact half-planes.

In the equivalent circuit description, we can characterize the slot diode with a two-dimensional electron channel by its impedance. Within the channel, the total current is the sum of the electron current and the displacement current caused by oscillating charges in both the channel and contacts of the diode. Far away from the slot, the current in the contact planes is purely conductive and is determined by the amplitude of the incident wave. Since the total current is conserved along the circuit, we can define the diode impedance  $Z = R + iX$  (per unit length of the slot) as

$$Z = \frac{1}{I} \int_{-w/2}^{w/2} E_x(x) dx,$$

where  $I = 2E_0/Z_0$  is the surface-current density induced by the incident wave in the perfectly conductive contact planes.

The frequency dependence of the diode's normalized impedance, shown in Fig. 2, displays resonances at plasmon excitation frequencies. The reactance  $X$  exhibits a transition from inductive ( $X < 0$ ) behavior, caused by the kinetic inductance of the electron channel, to a capacitive behavior ( $X > 0$ ) at the frequency of the fundamental plasmon resonance, which corresponds to the current resonance in the equivalent circuit description. However, no current resonance is exhibited at higher plasmon resonant frequencies.

The normalized resistance  $R/Z_0$  is, in essence, the matched width of the diode (measured along the slot), since the resistance of diode and the matched width is equal to the free-space impedance. The following theorem is valid:  $4R = Z_0 L^{(ex)}$ . The extinction length calculated using this formula (dashed curve in Fig. 1), and by Eq. (4) (solid line), coincides with the accuracy of our numerical procedure. Accordingly, we can introduce the electron resistance  $R_e$  and radiation resistance  $R_{rad}$ , where  $R_e = Z_0 L^{(ab)}/4$  and  $R_{rad} = Z_0 L^{(sc)}/4$ , respectively, so

that the total resistance of the diode is given by  $R = R_e + R_{\text{rad}}$ . Note that  $R$  does not vanish at high frequencies (but approaches  $R_{\text{rad}}$  instead).

One can see from Fig. 2 that the higher resonances are not nearly as pronounced as those predicted by the electrostatic description [15] because, at high frequencies, the  $R_{\text{rad}}C_g$  circuit shunts plasma oscillations in the channel effectively. However, a sharp fundamental resonance, which corresponds to the current resonance in the equivalent circuit description, shows up even for room temperature parameters of the diode.

The frequency of the fundamental plasma resonance in the slot diode increases as the slot width decreases (according to formula (5), it varies roughly as a square root of the inverse of the slot width). Figures 3 and 4 exhibit absorption length and scattering length spectra for a 100 nm width of the slot for different electron scattering rates. Notice that the resonant absorption (the absorption excess at the resonance over the nonresonant Drude background) grows considerably as the width of the slot decreases (cf. Figs. 1 and 3). Clearly, the fundamental plasma resonance becomes narrower when the electron scattering rate is decreased. However, the width of the resonance remains finite due to the radiative damping of plasma oscillations, even with no electron scattering in the channel. The width of the scattering resonance in the absence of electron scattering (see curve 4 in Fig. 4) originates entirely from radiative damping. To minimize an error arising from the nonresonant background contribution, we estimate the radiative damping of plasmons  $\gamma_{\text{rad}}$  as the half width at half magnitude (HWHM) in the low-frequency slope of the scattering-resonance curve for  $\nu = 0$  (curve 4 in Fig. 4), which yields  $\gamma_{\text{rad}} = 4.27 \times 10^{12} \text{ s}^{-1}$ . Then the electron scattering contribution to the resonance linewidth can be obtained as the difference between the HWHM measured in the low-frequency slope of the scattering resonance at any given  $\nu \neq 0$  (or, which yields the same result, in the high-frequency slope of the corresponding absorption resonance) and the radiative damping. The scattering length at the plasma resonance monotonically grows as the electron scattering rate decreases, while the resonant absorption exhibits a maximum when the dissipative broadening (caused by the electron scattering in the channel) of the resonance linewidth becomes equal to the radiative broadening (curve 2 in Fig. 3 corresponds to this case). The weaker, as well as the stronger, electron scattering result in a smaller resonant absorption. Note that under the condition of maximal absorption, the scattering length of the diode is approximately equal to its absorption length, which puts the limit of the diode's ratio of absorption to scattering length close to unity.

We conclude that a slot diode with a two-dimensional electron channel provides a resonant circuit at terahertz frequencies that effectively couples to external electromagnetic radiation with the loaded  $Q$ -factor exceeding unity, even at room temperature. We also

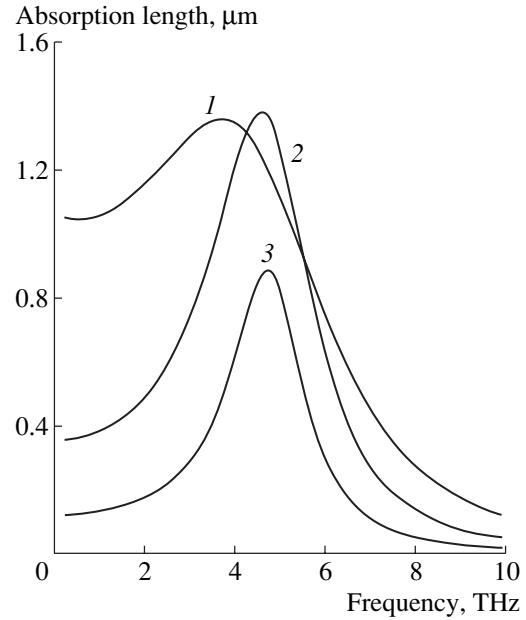


**Fig. 3.** Absorption length of the slot diode with the parameters  $N = 3 \times 10^{12} \text{ cm}^{-2}$ ,  $w = 0.1 \text{ μm}$ ,  $\epsilon_s = 13.88$ , and  $m^* = 0.042m_0$  as a function of the frequency for different electron scattering rates:  $\nu = 2 \times 10^{13} \text{ s}^{-1}$  (curve 1);  $7 \times 10^{12} \text{ s}^{-1}$  (curve 2);  $2.3 \times 10^{12} \text{ s}^{-1}$  (curve 3).

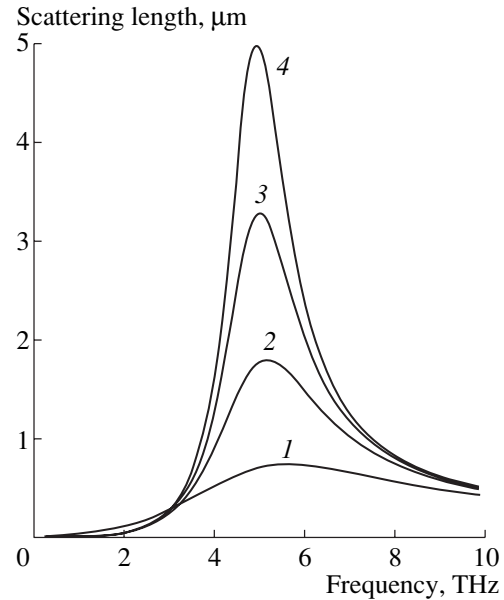


**Fig. 4.** Scattering length of the slot diode as a function of the frequency for different electron scattering rates:  $\nu = 2 \times 10^{13} \text{ s}^{-1}$  (curve 1);  $7 \times 10^{12} \text{ s}^{-1}$  (curve 2);  $2.3 \times 10^{12} \text{ s}^{-1}$  (curve 3);  $\nu = 0$  (curve 4). The other parameters of the diode are the same as those in Fig. 3.

claim that the diode's high-frequency resistance may be measured from contactless measurements of the characteristic electromagnetic lengths of the diode.

## ACKNOWLEDGMENTS

This work has been supported by the Russian Foundation for Basic Research, grant no. 03-02-17219, and by the Russian Academy of Sciences program “Novel Materials and Structures.” W.K. acknowledges the support of the CNRS-program “New THz Emitters and Detectors,” Region Languedoc Roussillon, and from the French Ministry of Research and New Technologies, program ACI “Nanosciences and Nanotechnologies.”

## REFERENCES

1. M. S. Shur and V. Ryzhii, in *Terahertz Sources and Systems*, Ed. by R. Miles, P. Harrison, and D. Lippens (Kluwer Academic, Dordrecht, 2001), p. 169.
2. M. Dyakonov and M. Shur, *Phys. Rev. Lett.* **71**, 2465 (1993).
3. M. Dyakonov and M. Shur, *IEEE Trans. Electron Devices* **43**, 380 (1996).
4. M. S. Shur and J.-Q. Lü, *IEEE Trans. Microwave Theory Tech.* **48**, 750 (2000).
5. W. Knap, V. Kachorovskii, Y. Deng, *et al.*, *J. Appl. Phys.* **91**, 9346 (2002).
6. W. Knap, Y. Deng, S. Rumyantsev, *et al.*, *Appl. Phys. Lett.* **80**, 3433 (2002).
7. X. G. Peralta, S. G. Allen, M. C. Wanke, *et al.*, *Appl. Phys. Lett.* **81**, 1627 (2002).
8. W. Knap, Y. Deng, S. Rumyantsev, and M. S. Shur, *Appl. Phys. Lett.* **81**, 4637 (2002).
9. V. V. Popov, O. V. Polischuk, T. V. Teperik, *et al.*, *J. Appl. Phys.* **94**, 3556 (2003).
10. V. V. Popov, T. V. Teperik, O. V. Polischuk, *et al.*, *Phys. Solid State* **46**, 153 (2004).
11. Y. Deng, R. Kersting, J. Xu, *et al.*, *Appl. Phys. Lett.* **84**, 70 (2004).
12. W. Knap, J. Lusakowski, T. Parenty, *et al.*, *Appl. Phys. Lett.* **84**, 2331 (2004).
13. A. V. Antonov, V. I. Gavrilenko, E. V. Demidov, *et al.*, *Phys. Solid State* **46**, 146 (2004).
14. P. J. Burke, I. B. Spielman, J. P. Eisenstein, *et al.*, *Appl. Phys. Lett.* **76**, 745 (2000).
15. V. Ryzhii, A. Satou, and M. S. Shur, *J. Appl. Phys.* **93**, 10041 (2003).
16. R. G. Newton, *Scattering Theory of Waves and Particles* (McGraw-Hill, New York, 1966; Mir, Moscow, 1969).
17. J. Alsmeier, E. Batke, and J. P. Kotthaus, *Phys. Rev. B* **40**, 12574 (1989).